Self-assembled Au nanoparticles arrays by porous anodic alumina oxide and optical properties

Wang Yingwei[1], Wang Fei[1,2], Fu Liping[1], Fang Jingyue[2], Wang Guang[2], Chang Shengli[2], Zhang Xueao[2]

(1. College of Physics and Electronics, Central South University, Changsha 410073, China;
2. College of Science, National Defense Technology University, Changsha 410073, China)

Abstract: Using vacuum deposition and subsequent thermal dewetting, Au nanoparticles ordered array were fabricated on the conventional ordered porous alumina template. Here, a self-assembled two-dimensional Au nanoparticles arrays was demonstrated, which consisted of several gold nanoparticles around every hole on the surface of porous alumina template. Furthermore, second anodized and widen diameter time influence on templates formed were investigated. During the fabrication of template, first anodization played guiding role for second anodization, and the diameter of hole direct was proportion with the widen diameter time. It also found that the form of Au nanoparticles arrays depend on the thickness of Au film. At last, optical properties for the material was test. Strong absorption peaks of the UV-visible absorption spectrum due to the surface plasmon resonance of Au nanoparticles were observed.

Key words: gold nanoparticles arrays; self-assembled; anodic alumina oxide(AAO); surface plasmon resonance(SPR)

CLC number: TB133 Document code: A Article ID: 1007-2276(2013)11-3047-06

介孔氧化铝组装金纳米颗粒阵列及其光学性质

王迎威[1],王 飞[1,2],符力平[1],方靖岳[2],王 广[2],常胜利[2],张学骜[2]

(1. 中南大学 物理与电子学院, 湖南 长沙 410073;
2. 国防科学与技术大学 理学院, 湖南 长沙 410073)

摘 要:采用真空蒸镀的方法在多孔氧化铝模板表面得到薄金膜,随后在真空管式炉中进行热处理,热处理中发生的热去湿过程使得金膜在多孔氧化铝表面形成有序的金纳米颗粒阵列。同时还研究了多孔氧化铝模板制备过程中二次氧化的作用,发现一次氧化对二次氧化进行具有一定指导作用;另外,研究了扩孔时间对模板孔径的影响,一定条件下,扩孔时间与孔径成正比例关系;最后研究了镀膜厚度对金纳米颗粒的影响,结果中可以看到,金膜的厚度直接影响金纳米颗粒阵列的形成。最后在分光光度计上的光学测量吸收光谱的结果中,出现了表面等离子体作用引起的很强的吸收峰。

关键词:金纳米颗粒阵列; 自组装; 阳极氧化铝; 表面等离子体

收稿日期:2013-03-10; **修订日期**:2013-04-11

基金项目:国家自然科学基金(11104349);校预研项目(JC13-02-14)

作者简介:王迎威(1988-),男,硕士生,主要从事纳米材料方面的研究工作。Email:wangyignwei1988@126.com

通信作者:王飞(1981-),男,讲师,从事纳米材料制备、组装及器件研究。Email:wangfei_815@163.com

导师简介:张学骜(1977-),男,博士生导师,长期从事纳米材料制备及改性的研究工作。Email:xazhang@nudt.edu.cn

0 Introducton

Nano-structures made of noble metals have attracted much interest during the past decades due to their wide use in many areas, such as in catalysis [1-2], sensing [3-5], data storage [6] and biological related region [7]. Ordered metal nanoparticles arrays always perform dramatic properties, especially optical characteristics. In recent years, self-assembled Au nanoparticles have been widely studied in localized surface plasmon resonance (LSPR) [8-9], surface-enhanced raman scattering (SERS) [10-12] and metal-enhanced fluorescence (MEF) [13]. Simultaneously, various self-assembled methods have been develeped, such as placement using physical templates [14-16] self-assembled monolayers [17-18] electrostatic templates [19-20] DNA-programmed [21-23] and other strategies [24]. While the challenge remains of obtaining an ordered array over a large area. Here, we dem onstrated the large area fabricaton of Au nanoparticles array in low cost, high throughput and high efficiency. Porous anodic alumina oxide was ideal self-assembled templates as reported previously [25-27]. First, we got self-assembled templates with 80 nm diameter and 20 nm wall-thickness by conventional fabrication technology. Then, the deposition of a thin gold film onto substrates by vacuum deposition, and followed thermal annealing in tube furnace. In this paper, we investigated several influence factors during the fabrication of self-assembled templates and the effect of thickness on nanoparticle array formation. The fabricated nanostructures exhibit excellent optical absorption properties, which are important for many plasmonics applications. It also demonstrated a very simple technique for rapid and large-scale assemble of nanoparticles.

1 Experiment

1.1 Materials

The film of high-purity aluminum (99.999%, 0.5 mm thickness), spun gold (99.999%, 0.3 mm diameter), acetone, ethanol, perchloric acid, oxalic acid, sodium hydroxide, phosphoric acid and chromium trioxide. All chemicals are used as received without furture purification.

1.2 Fabrication of porous anodic alumina oxide

Prior to anodizing, high-purity aluminum foils was annealed under nitrogen atmosphere at 500 °C for 4 h. The tailored polished foils of a square area 2 cm^2 degreased in acetone and washed in absolute alcohol and deionized water successively. Subsequently, the foils were electropolished in a 1:4 volume mixture of perchloric acid and ethanol at 16 V voltage at 20 ℃ to diminish the roughness of the alumina foils surface.

Ordered porous anodic alumina oxide were prepared through two-step anodizing electrochemical procedure. Tailor-made square aluminum foils was used as anode and graphite sheet as cathode, and 0.3 M oxalic acid as the electrolyte. The experimental electrolyte temperature was maintained at 14 ℃, while the temperature deviated from that value by less than 0.1 °C (used low temperature thermostat bath). The anodization voltage was maintained a constant of 40 V direct current (dc) potential. The first anodization carried out for 6 h at above conditions. It was produced that thick layer of porous aluminum oxide consisting of an array of vertically arranged pores on the surface of aluminum. Then the foils were soaked in in chromic (1.8%)-phosphoric (6%) acid solution for about 12 h. Under the same experimental conditions, the second anodization carried out for 2 h. This two-step anodizing electrochemical procedure produced hexagonally ordered nanoporous layer with pore diameter about 30 nm. The diameter was not large enough for self-assembed Au nanoparticles. Consequently, the anodized foil was soaked in 5% phosphoric acid for about 80 min at 20 ℃. The nanopore diameter of template was widen from 30 to 80 nm.

1.3 Vacuum deposition and thermal annealing

The prepared template was cleaned and dry. Film

of gold was deposited on the surface of template, which was 10、20、30 nm thickness. Thermal annealing for the dewetting process was done in a tube furnace at the condition of 550 ℃ for 3 h under N_2 environment. The deposited was done by vacuum deposition apparatus.

2 Results and discussion

2.1 Second anodization influence on templates

The microstructure of templates were characterized by scanning electron microscopy. Figure 1 (a) shown the surface of template, which was anodized just once. The regularity of templates obtained by first anodized was poor and there were many defects on the surface. In the case of second anodization, the perfect close-packed hexagonal pore array was fabricated(Figure 1(b)).

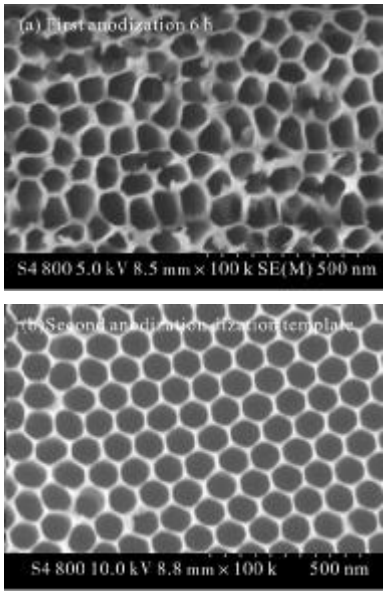

Fig.1 SEM of porous anodic alumina oxide

According to the model that describes the self-regulating pore growth [28], the formation of surface random microcracks is precondition for close-packed hexagonal pore array. The random microcracks formed at anodize prophase lead toinevitable surface defect region. Before second anodization, the templates was soaked into chromic-phosphoric acid solution for long time. The result in highly ordered pits arise on the surface of alumina. Such pits was producted during the first anodized by barrier layer. When the second anodization begun, anodization take place in these pits at first. During this process these pits play a guiding role [29]. Finally, the close-packed hexagonal pore array was fabricated.

2.2 Time of widen nanopore effect on diameter of nanopore

In order to obtain templates which had 80 nm diameter and 20 nm wall thickness, the nanopore diameter was widen from 30 nm to 80 nm after second anodization. Template was soaked in 5% phosphoric acid for 0 min, 60 min, 80 min, 120 min at 20℃. The SEM images shown in Figure 2 (a). The diameter of

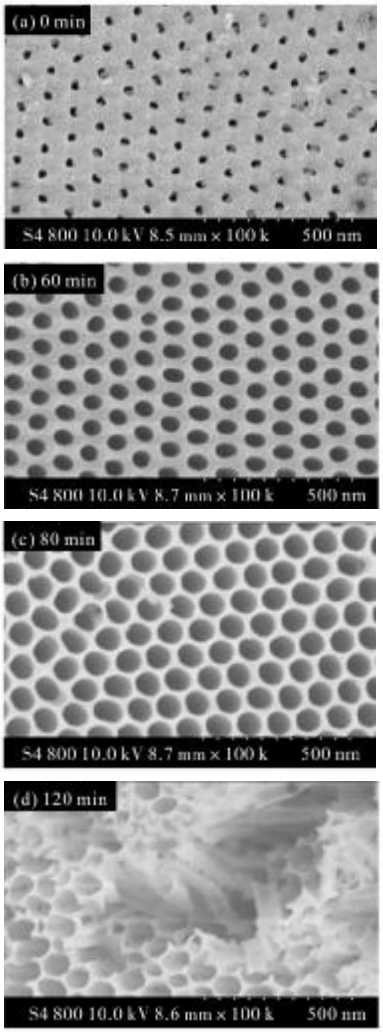

Fig.2 SEM of templates for different widen pore time at 20℃ [first andized 6 h, soaked in admixture acid 12 h, second andized 2 h, 40 V, 0.3 M $(COOH)_2$, 14 ℃]

pore was approximately 30 nm which not treatment with phosphoric acid. After widen diameter for 60 min, it was widen form 30nm to 60nm (Figure 2 (b)). With the soaking duration, the diameter of nanopore became larger. Highly ordered nanopore arrays are acquired when the soaking time increased to 80 min(Figure 2(c)). But the wall began to collapse between adjacent holes when the time up to 120 min (Figure 2 (d)). We found that the diameter of hole direct proportion with the widen diameter time. The dependence of diameter on the widen diameter time was given in Fig. 3. The linear relationship was obvious and the rate about 1 nm/min. Such law were useful for the preparation of tunable diameter templates.

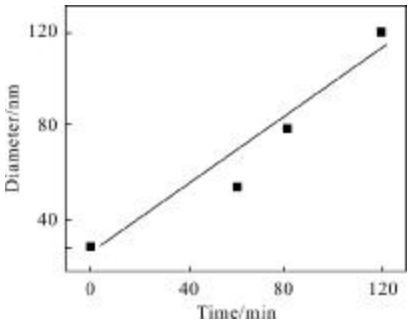

Fig.3 Variation of template pore diameter with time of widen pore

2.3 Gold thickness effect on self-assembled Au nanoparticles array

we deposited gold film on the surface of template, as discussed in experimental section. As can be seen, approximate triangle area is formed among three adjacent hole which were covered with gold film. As a result the triangle gold patches were generated. Subsequently, a dewetting process [30-32] of the gold film occured in each triangle area during thermal annealing. The temperature of thermal annealing was 550℃ for 3 h. As shown in Figure 4(a), the Au nanostructures prepared using spun gold 4 cm during vacuum deposition, in this condition there were not clear Au nanoparticles formed. We believed that the extremely thin gold films acts as an obstacle for big Au nanoparticle formation. Nanoparticle arrays were acquired around the hole correspond to use 8 cm spun gold in the Figure 4 (b). In the case, the film was initially too thick used 12 cm spun gold, nanoparticles array exhibited dramatic change, which showed in the Fig. 4 (c). Large quantity big particles dispersed in the template surface randomly. This is consistent with previous reports[33].

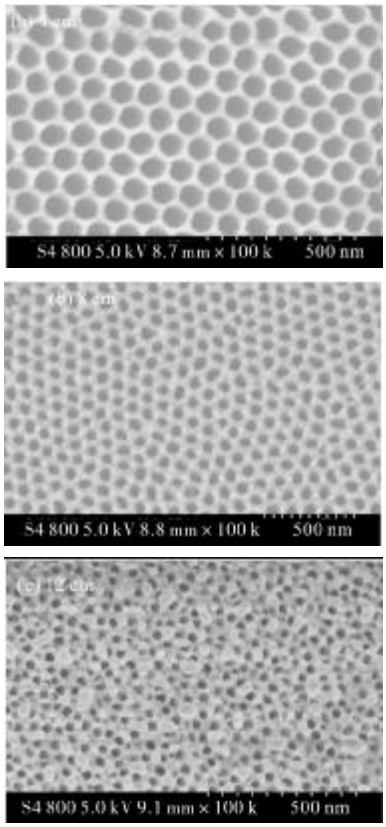

Fig.4 SEM images of self-assembled Au nanoparticles formed under different spun gold depletion length during vacuum deposition

2.4 Optical properties investigations for Au nanoparticles array

Figure 5 showed the representative curve of the light absorption with respect to different samples for the light excitation 15°. The black line represented the absorption curve of ordinary template. Double resonance frequencies were revealed. Between 800 nm and 900 nm we observed first peak. Furthermore, the second peak appeared nearby 1 400 nm. Red line demonstrated the absorption curve for the samples after vacuum deposition and thermal annealing. There were three peak was observed. The second peak and third peak corresponded to ordinary template absorption

spectra. In the preliminary analysis of expermental data, we found that the first peak at 526 nm consistent with the absorption peak of Au nanoparticles, which could be described by Mie-scattering theory.

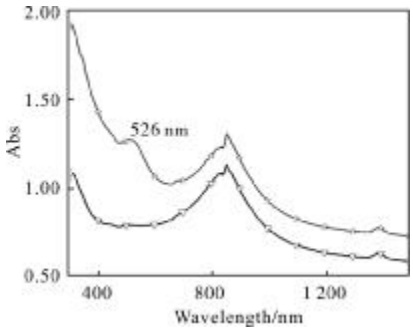

Fig.5 Absorption spectra of ordinary template(-☆-) and template with self-assembled Au nanoparticles(-▽-)

3 Conclusion

In summary, first, we found that first anodization played a guiding role for the second anodization during preparation of templates. The regularity of templates performed perfectly close-packed hexagonal pore array which fabricated by second anodization. Second, the ideal nanopore array of 80 nm diameter and 20 nm thin nanowalls could be abtained with the time 80 min at 20 ℃. It known that the speed of widen diameter was about 1 nm/min at 20 ℃. Third, the thickness of Au film influences the form of Au nanoparticle. When 8 cm thickness of Au film was consumption during vacuum deposition, Au nanopaticle arrays were obtained. Finally, the absorption characteristics caused by surface plasmon resonance were observed. For ordinary templates, there were two absorption peak near-infrared region. While, typical absorption peak (526 nm) for Au nanoparticle was observed in visible region. Futuremore, we would try to self-assembed Au nanoparticle in shallow nanopore by porous anodic alumina oxide, which are expected to demonstrate excellent surface plasmon resonance.

References:

[1] Mahmoud M A, Saira F, ElSayed M A. Hollow nanoparticles [J]. Nano Lett, 2010, 10: 3764-3769.

[2] Zeng J, Zhang Q, Chen Y, et al. Comparison study of the catalytic properties of Au-based nanocages nanoboxes and nanoparticles [J]. Nano Lett, 2010, 10: 30-35.

[3] Hyunhyub Ko, Srikanth S, Vladimir V T. Nanostructured surfaces and assemblies as SERS media [J]. Small, 2008, 4: 1576-1599.

[4] Tripp R A, Dluhy R A, Zhao Y P. Novel nanostructuresfor SERS biosensing[J]. Nano Today, 2008, 3: 31-37.

[5] Smith W E. Practical understanding and use of surface enhanced Raman scatteringsurface enhanced resonance Raman scattering in chemical and biologicalanalysis [J]. Chem Soc Rev, 2008, 37: 955-964.

[6] Hong A J, Liu C C, Wang Y, et al. Metal nanodot memory by Self-assembled block copolymer lift-off [J]. Nano Lett, 2010, 10: 224-229.

[7] Giljohann D A, Seferos D S, Daniel W L, et al. Gold nanoparticles for biology and medicine [J]. Angew Chem Int Ed, 2010, 49: 3280-3294.

[8] Lukyanchuk B, Zheludev B I, Maier S A, et al. The Fano resonance in plasmonic nanostructuresand metamaterials [J]. Nat Mater, 2010, 9: 707-715(2010).

[9] Le F, Brandl D W, Urzhumov Y A, et al. Metallic nanoparticle arrays: a common substrate for both surface-enhanced Raman scattering and surface-enhanced infrared absorption[J]. ACS Nano, 2008, 2: 707-718.

[10] Stiles P L, Dieringer J A, Shah N C, et al. Surface-enhanced Raman spectroscopy [J]. Annu Rev Anal Chem, 2008, 1: 601-626.

[11] Yao J Q, Di Z G, Jia C G, et al. Photonic crystal fiber SERS sensors[J]. Infrared and Laser Engineering, 2011, 40: 96-106.

[12] Fan X G, Wang X, Xu Y J, et al. Design of Raman spectroscopy measurement system based on SHINERS [J]. Infrared and Laser Engineering, 2013, 42: 1798-1803.

[13] Aouani H, Wenger J, Gerard D, et al. Crucial role of the adhesion layer on the plasmonic fluorescence enhancement[J]. ACS Nano, 2009, 3: 2043-2048.

[14] Xia Y N, Yin Y D, Lu Y, et al. Template-assisted self-assembly of spherical colloids into complex and controllable structures[J]. Adv Funct Mater, 2003, 13: 907-918.

[15] Yin Y D, Lu Y, Xia Y N. A self-assembly approach to the formation of asymmetric dimers from monodispersed spherical colloids[J]. J Am Chem Soc, 2001, 123: 771-772.

[16] Zhong Z Y, Bauer G. Site-controlled and size-homogeneous Ge islandson prepatterned Si (001) substrates [J]. Appl Phys Lett, 2004, 84: 1922-1924.

[17] Liu S T, Maoz R, Sagiv J. Planned nanostructures of colloidal gold via self-assembly on hierarchically assembled organic bilayer template patterns with in-situ generated terminal amino functionality[J]. Nano Lett, 2004, 4: 845-851.

[18] Wang Y H, Maspoch D, Zou S L, et al. Controlling the shape orientation and linkage of carbon nanotube features with nano affinity templates. Proc Natl Acad Sci USA. 103: 2026-2031 (2006).

[19] Jacobs H O, Whitesides G M. Submicrometer patterning of charge in thin-film Electrets[J]. Science, 2001, 291: 1763-1766.

[20] Cao T B, Xu Q B, Winkleman A, et al. Fabrication of thin metallic films along the sidewalls of a topographically patterned stamp and their application in charge printing [J]. Small, 2005, 1: 1191-1195.

[21] Seeman N C. DNA in a material world [J]. Nature, 2003, 421: 427-431.

[22] Yan H, Park S H, Finkelstein G, et al. DNA-templated self-assembly of protein arrays and highly conductive nanowires[J]. Science, 2003, 301: 1882-1884.

[23] Le J D, Pinto Y, Seeman N C, et al. DNA-templated self-assembly of metallic nanocomponent arrays on a surface [J]. Nano Lett, 2004, 4: 2343-2347.

[24] Koh S J. Strategies for controlled placement of nanoscale building blocks[J]. Nanoscale Res Lett, 2007, 2: 519-545.

[25] Huber C A, Huber T E, Sadoqi M, et al. Nanowire array composites [J]. Science, 1994, 263: 800-802.

[26] Losic D, Shapter J G, Mitchell J G, et al. Fabrication of gold nanorod arrays by templating from porous alumina [J]. Nanotechnology, 2005, 16: 2275-2281.

[27] Li C P, Roshchin L V, Viret M, et al. Fabrication and structural characterization of highly ordered sub-100-nm planar magnetic nanodot arrays over 1 cm^2 coverage area[J]. J Appl Phys, 2006, 100: 074318.

[28] Parkhutik V P, Shershulsky V I. Theoretical modelling of porous oxide growth on aluminium [J]. J Phys D: App Phys, 1992, 25: 1258-1263.

[29] Zhu Xufei, Han Hua, Qi Weixing, et al. Theoretical foundation and limitation of two-step anodizing technology [J]. Process in Chemistry, 2012, 24(11): 2073-2086.

[30] Bischof J, Scherer D, Herminghaus S, et al. Dewetting modes of thin metallic films: Nucleation of holes and spinodal dewetting[J]. Physical Review Letters, 1996, 77:1536-1539.

[31] Thiele U, Mertig M, Pompe W. Dewetting of an evaporating thin liquid film: heterogeneous nucleation and surface instability[J]. Physical Review Letters, 1998, 80: 2869-2872.

[32] Yang S K, Cao B Q, Kong L C, et al. Template-directed dewetting of a gold membrane to fabricate highly SERS-active substrates[J]. J Mater Chem, 2011, 21: 14031-14035.

[33] Giermann A L, Thompson C V. Solid-state dewetting for ordered arrays of crystallographically oriented metal particles [J]. Applied physics letters, 2005, 86: 121903.